

# Tailoring of Optoelectronic Properties of InAs/GaAs Quantum Dot Nanosystems by Strain Control

Woong Lee,<sup>1</sup> Keesam Shin,<sup>1</sup> and Jae-Min Myoung<sup>2,\*</sup>

<sup>1</sup>School of Nano & Advanced Materials Engineering, Changwon National University,  
9 Sarim-dong, Changwon, Gyeongnam 641-773, Republic of Korea

<sup>2</sup>Dept. of Materials Science and Engineering, Yonsei University,  
134 Shinchon-dong, Seoul 120-749, Republic of Korea

Full three-dimensional numerical analysis based on continuum elasticity and model solid theory has been carried out to evaluate some possible means of tailoring the optoelectronic properties of InAs/GaAs quantum dot (QD) nanosystems. Numerical results predicted that while the stacking period control leads to the shifts in valence band edges, incorporation of In<sub>x</sub>Ga<sub>1-x</sub>As ternary strain relief layer (SRL) causes composition-dependent shifts in conduction band edges. On the other hand, modification of the SRL shape itself did not yield significant changes in the confinement potentials. It is therefore suggested that strain control by incorporation of ternary intermediate layers combined with geometry controls, would allow greater flexibility in the tailoring of the opto-electronic characteristics of QD-based systems.

**Keywords:** quantum dot, bandgap engineering, strain control, photovoltaics

## 1. INTRODUCTION

In quantum dot (QD) nanosystems, countable number of carriers are three-dimensionally confined in small space to yield  $\delta$ -function-like density of states leading to the improved efficiencies in light emission and absorption due to fully quantized atom-like excitonic behaviours.<sup>[1]</sup> This endows QD systems with promising application potentials to the components of future optoelectronic devices. Among the many possible material combinations, InAs QD/GaAs matrix systems have been intensively studied for 1.2 – 1.5  $\mu$ m wave infrared (IR) applications.<sup>[2]</sup> Another potential application of this system is the third-generation photovoltaic devices for renewable energy sources<sup>[3]</sup> and long-wavelength IR detection systems<sup>[4]</sup> with substantially improved conversion efficiencies. In these systems, it is desirable to tailor the energy band structures for design flexibility, i.e. wider operation wavelength ranges, in addition to the unique characteristics due to the 3-D confinement of carriers.

One attractive approach to bandgap engineering is the control of strains. In QD systems, inherent strains due to the mismatch in lattice parameters between the QD and the matrix materials may develop in various ways depending on geometry, composition and/or materials combinations<sup>[5,6]</sup> while strains are known to modify energy band structures of

solids.<sup>[7]</sup> These characteristics make it possible for strains in QD systems to be ‘controlled,’ allowing some degree of freedom in designing QD systems with tailored opto-electronic properties. For such strain-modified bandgap controls, it is necessary to understand how strain fields are modified in QD systems through changes in either geometric or materials parameters and thereby predict resulting the profiles of the confinement potentials.

In this study, some candidate methods for strain-controlled bandgap engineering of InAs/GaAs QD systems are evaluated within the framework of three-dimensional continuum elasticity and eight-band  $\mathbf{k}\cdot\mathbf{p}$  theory to obtain systematic understanding of the modifications of band edge profiles with varying geometry and compositions of stacked multi-layer QD systems. Two possible cases are considered: i) InAs QD/GaAs spacer systems with ternary In<sub>x</sub>Ga<sub>1-x</sub>As intermediate layers having various In concentrations,  $x$  in which inter-dot spacing is varied; and ii) similar system with varying ternary layer shape. Considering the dimensions of QD systems, atomistic method may be used to calculate strains<sup>[8]</sup> and for the analysis of the stacked QD systems, two-dimensional models have been adopted assuming axi-symmetric geometry.<sup>[9,10]</sup> However, these methods have limitations in computational cost or in fully considering orientation-dependent properties if the shape of the QD system deviates from circular-symmetry with respect to the QD axis. Therefore, the numerical results in this study would have direct correlations to the real QD systems.

\*Corresponding author: jmyoung@yonsei.ac.kr

## 2. NUMERICAL ANALYSIS

Figure 1 shows the geometry and dimension of the five-layer stacked QD structure modelled for the FE analysis together with the FE meshing. Based on the experimentally observed shapes of InAs QDs in GaAs matrix,<sup>[11-13]</sup> it was assumed in the current study that QDs have a lens-like shape in the current study. Considering the cubic anisotropy of the constituent materials and the geometric symmetry of the system, only the quarter section of the whole structure was modelled. The GaAs cap and buffer layers were both chosen to be 30 nm thick to represent QDs embedded in sufficiently thick matrices. The lateral periodicity of the structure was assumed to be 60 nm while the vertical stacking period  $P$  was varied between 5.5 to 10 nm. Elastic constants of the constituent materials listed in Table 1<sup>[7]</sup> were applied to the FE model. The lattice mismatch strains between the InAs QD, GaAs matrix and  $\text{In}_x\text{Ga}_{1-x}\text{As}$  ternary layer (for the FE models with ternary layers incorporated) were simulated using an analogy of thermal misfit strain and ‘cut-and-weld technique’.<sup>[14]</sup> Twenty-node quadratic brick elements were employed for meshing. A general-purpose finite element analysis package ABAQUS (Hibbitt, Karlsson & Sorensen, Inc.) was used for calculations.

Using the strain information obtained from the FE analysis, band edge profiles were estimated within the framework of 8-band  $\mathbf{k}\cdot\mathbf{p}$  theory. Taking the weight-average over the three uppermost valence bands at Brillouin zone centre ( $k=0$ ) as a reference energy level  $E_{v,av}^0$ , strain-modified edges of

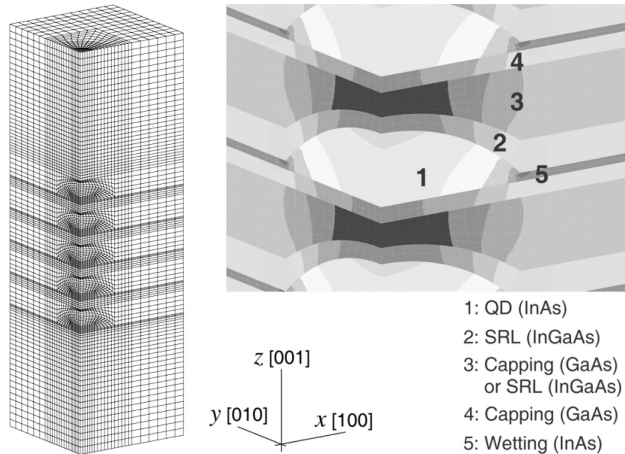


**Fig. 1.** Geometry model and finite element (FE) meshes for the analysis of strains.

**Table 1.** Elastic properties of single crystalline InAs, GaAs and  $\text{In}_x\text{Ga}_{1-x}\text{As}$  used for the numerical analysis

Material	$C_{11}$ (GPa)	$C_{12}$ (GPa)	$C_{44}$ (GPa)
InAs	83.29	45.26	39.60
GaAs	118.8	53.76	59.40
$\text{In}_x\text{Ga}_{1-x}\text{As}$	$118.8 - 35.51x$	$53.76 - 8.5x$	$59.4 - 19.8x$

the conduction band  $E_c$ , heavy-hole valence band  $E_v^{\text{hh}}$  and light-hole valence band  $E_v^{\text{lh}}$  are expressed as:<sup>[7]</sup>

$$E_c = E_{v,av}^0 + \frac{\Delta_0}{3} + E_g + E_c \quad (1)$$

$$E_v^{\text{hh}} = E_{v,av}^0 + \frac{\Delta_0}{3} + \delta E_{v,\text{hyd}} - \frac{1}{2} \delta E_{v,\text{sh}} \quad (2)$$

$$E_v^{\text{lh}} = E_{v,av}^0 - \frac{\Delta_0}{6} + \delta E_{v,\text{hyd}} + \frac{1}{4} \delta E_{v,\text{sh}} + \frac{1}{2\sqrt{\Delta_0^2 + \Delta_0 \delta E_{v,\text{sh}} + \frac{9}{4} (\delta E_{v,\text{sh}})^2}} \quad (3)$$

where  $\Delta_0$  is the spin-orbit splitting in the unstrained state and  $E_g$  is the bandgap. Strain-induced modifications of band edges due to various strain components  $\delta E_c$ ,  $\delta E_{v,\text{hyd}}$  and  $\delta E_{v,\text{sh}}$  are given by:<sup>[7]</sup>

$$\delta E_c = a_c(\epsilon_{xx} + \epsilon_{yy} + \epsilon_{zz}) = a_c \epsilon_{\text{hyd}} \quad (4)$$

$$\delta E_{v,\text{hyd}} = a_v(\epsilon_{xx} + \epsilon_{yy} + \epsilon_{zz}) = a_v \epsilon_{\text{hyd}} \quad (5)$$

$$\begin{aligned} (\delta E_{v,\text{sh}})^2 &= \frac{b^2}{2} [(\epsilon_{xx} - \epsilon_{yy})^2 + (\epsilon_{yy} - \epsilon_{zz})^2 + (\epsilon_{zz} - \epsilon_{xx})^2] \\ &+ d^2 (\epsilon_{xy}^2 + \epsilon_{yz}^2 + \epsilon_{zx}^2) \end{aligned} \quad (6)$$

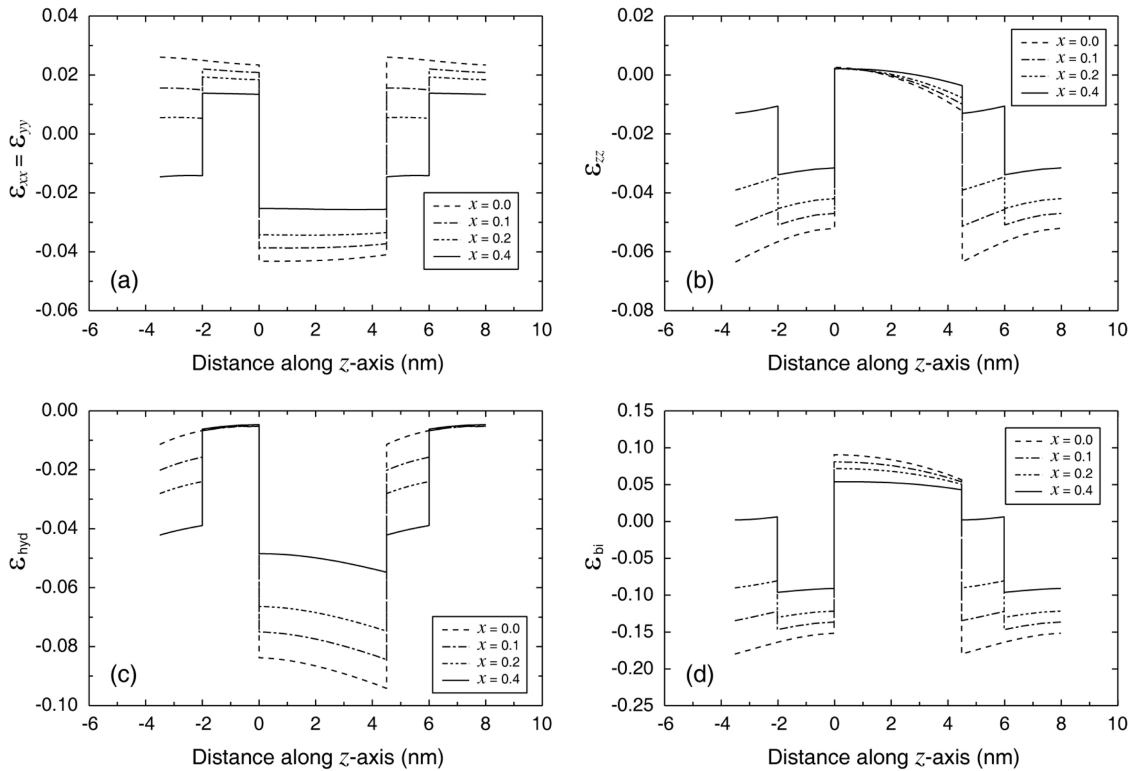
where  $a_c$ ,  $a_v$ ,  $b$  and  $d$  are deformation potentials. Material constants for the estimations of the strain-modified band edge profiles *via* Eqs. 1 through 6 are listed in Table 2.

## 3. RESULTS AND DISCUSSION

Effect of the introduction of  $\text{In}_x\text{Ga}_{1-x}\text{As}$  ternary layers, having intermediate lattice parameter values between GaAs and InAs, on the modification of the strains in the QD structure is clearly visible in Fig. 2 in which various strain components are plotted along the  $z$ -axis for  $P=8$  nm. As the In concentration,  $x$ , increases from 0 to 0.4, substantial relaxation of strains in the QD region ( $0 < z < 4.5$  nm) is predicted for the lateral component  $\epsilon_{xx}$ . On the other hand, relaxation of the vertical strain component  $\epsilon_{zz}$  within the QD region is somewhat limited, whereas  $\epsilon_{zz}$  in the surrounding regions ( $4.5 < z < 6$  nm) are significantly relaxed with increasing  $x$ . Since the InGaAs ternary layer is located between spacers, it is strained like a quantum well or thin film throughout most of its volume as it contracts in lateral directions to conform to the GaAs spacer ( $6 < z < 8$  nm) to maintain atomistic continuity across the interface. Then, lateral contraction of the ternary layer yields corresponding vertical expansion, effectively reducing vertical misfit strain at the interface with the QD (reduced  $\epsilon_{zz}$ ). At the same time, with increasing  $x$ , lattice parameter of the ternary layer becomes closer to that of the InAs QD as well. Therefore, the vertical strain in the QD would not change significantly with the varying In concen-

**Table 2.** Band structure parameters of InAs, GaAs and  $\text{In}_x\text{Ga}_{1-x}\text{As}$  used to estimate strain-induced changes of confinement potentials

Parameters	InAs	GaAs	$\text{In}_x\text{Ga}_{1-x}\text{As}$
$a$ (Å)	6.0553	5.6503	$5.6503 + 0.405x$
$E_{v,av}^0$ (eV)	-6.67	-6.92	$-6.92 + 0.231x - 0.058x^2$
$E_g$ (eV)	0.354	1.424	$0.354 + 0.7(1-x) + 0.4(1-x)^2$
$\Delta_0$ (eV)	0.38	0.34	$0.340 - 0.093x + 0.133x^2$
$a_c$ (eV)	-5.08	-8.01	$-8.01 + 2.93x$
$a_v$ (eV)	1.00	1.16	$1.16 - 0.16x$
$b$ (eV)	-1.8	-1.7	$-1.7 - 0.1x$
$d$ (eV)	-3.6	-4.55	$-4.55 + 0.95x$

**Fig. 2.** Profiles of strain components in the mid-layer of the stacked QD structure with incorporated ternary layer: (a)  $\epsilon_{xx}$  ( $=\epsilon_{yy}$ ), (b)  $\epsilon_{zz}$ , (c)  $\epsilon_{hyd}$  and (d)  $\epsilon_{bi}$  along the  $z$ -direction through the symmetry axis.

tration of the ternary layer. However, the small volume of the ternary layer just above the QD has to expand laterally to conform to the QD having the larger lattice parameter. Simultaneously, the spacer region between the ternary layer and the QD is also strained in tension to conform to the QD. Hence, the thin ternary layer region just above the QD is under compressive vertical strain to counterbalance the lateral stretch (tensile strain) and this vertical compressive strain is relaxed with increasing  $x$ , *i.e.* there are reduced differences in the lattice parameters between the QD and the ternary layer.

Such strain modifications due to the InGaAs ternary layer result in the relaxation both of hyd and bi with increasing  $x$ . As the changes in  $\epsilon_{xx}$  ( $=\epsilon_{yy}$ ) are not compensated by  $\epsilon_{zz}$ , com-

positional variations in the ternary layer cause significant changes in hyd as shown in Fig. 2(c). At the same time, relatively smaller changes in  $\epsilon_{zz}$  yields the reduced range of the changes in  $\epsilon_{bi}$  with varying ternary layer composition (Fig. 2(d)). In the case of  $\epsilon_{bi}$ , strain relaxation is somewhat more significant near the dot base ( $z = 0$  nm) with higher In concentration. In the ternary layer region ( $4.5 < z < 6.0$  nm), strain relaxations occur in such a way to reduce height of ‘strain step’ at the QD/ternary layer interface ( $z = 4.5$  nm) with a higher In concentration.

The significance of the results shown in Fig. 2 is that the incorporation of the ternary layer yields change in hyd, which has been almost unattainable through the geometry

control alone, e.g. QD shapes<sup>[6]</sup> and stacking period.<sup>[9]</sup> The controllability of hyd implies that the conduction band edges of the QD structure can now be modified by varying the composition of the InGaAs ternary layer. In order to visualise this possibility, band edge profiles are plotted in Fig. 3(a) as functions of distance along the  $z$ -direction for various In concentrations,  $x$ , in the ternary layer. In this plot, light-hole band edges are omitted for readability as they were predicted to be at lower energy positions than the heavy-hole band edges. It can be seen that the effect of the relaxation of hyd, shown in Fig. 2(c), is well reflected in the strain-modified conduction band edges shifting toward lower energy positions. In contrast, the effects of relaxed strains are almost unappreciable in the profiles of the valence band edges, reflecting relatively smaller changes of  $\epsilon_{bi}$  with varying  $x$ .

Similar analysis has been carried out for other stacking periods and the estimated band edge energies at the QD bases ( $z=0$  nm) for various In concentrations are plotted in Fig. 3(b) for conduction band edges, heavy-hole valence band edges and light-hole valence band edges, respectively, as functions of stacking periods. It is clear that an increase in In concentration,  $x$ , within the  $\text{In}_x\text{Ga}_{1-x}\text{As}$  ternary layer lowers the conduction band edge substantially whereas the heavy-hole band edge is almost insensitive to  $x$ , resulting in decreasing bandgap energy with higher  $x$ . In addition, no Type-II transition is expected for all the stacking periods considered herein as the light-hole band edges in the GaAs spacer are below the heavy-hole band edges in the InAs QD.

These predictions imply that introduction of the InGaAs ternary layer increases the flexibility in bandgap engineering since the conduction band, where potential well is deeper than the valence band, can be tailored.

In order to further explore the possible means of bandgap engineering, effect of the shape of the ternary layer was considered and the results are shown in Fig. 4. Figures 4(a) through (c) shows the band edge profiles obtained for the configurations shown in the lower right drawing with corresponding labels. Comparison of Fig. 4(a) and (b) indicates that changes in the shape of the ternary layer from a well type to a cladding type would result in the shift of both the conduction band edges and the valence band edges. On the other hand, it is predicted from Figs. 4(b) and (c) that minor changes in the cladding geometry itself does not yield any noticeable modifications of the band edge profiles. These results imply that thin cladding type ternary layer may not be sufficient to 'shield' the influence of the GaAs capping layer. However, modification of the shape of the ternary layer between the well type and the cladding type does modify the band edge profiles, possibly by changing the amount of the shielding the influence of the capping layer on the strain field within the QD.

From the results shown in Figs. 2 through 4, it can be inferred that wider controllability of the band structures of QD systems could be achieved by combining two approaches, i.e. modification of the conduction band by the incorporation of ternary layer with varying composition and some modifi-

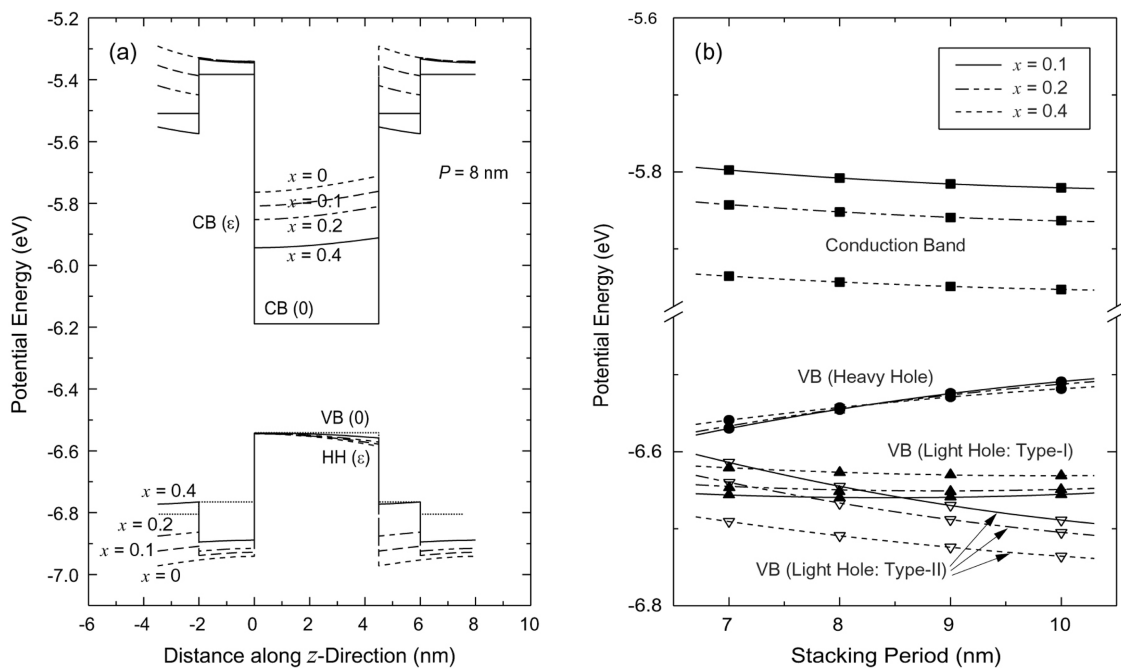


**Fig. 3.** (a) Strain-modified confinement potentials along the  $z$ -direction in and around the QD in the mid-layer of the stacked multi-layer structure with ternary layers and (b) band edge energies at the dot bases ( $z=0$ ) plotted as functions of In concentration,  $x$ , in the ternary layer and of stacking period.

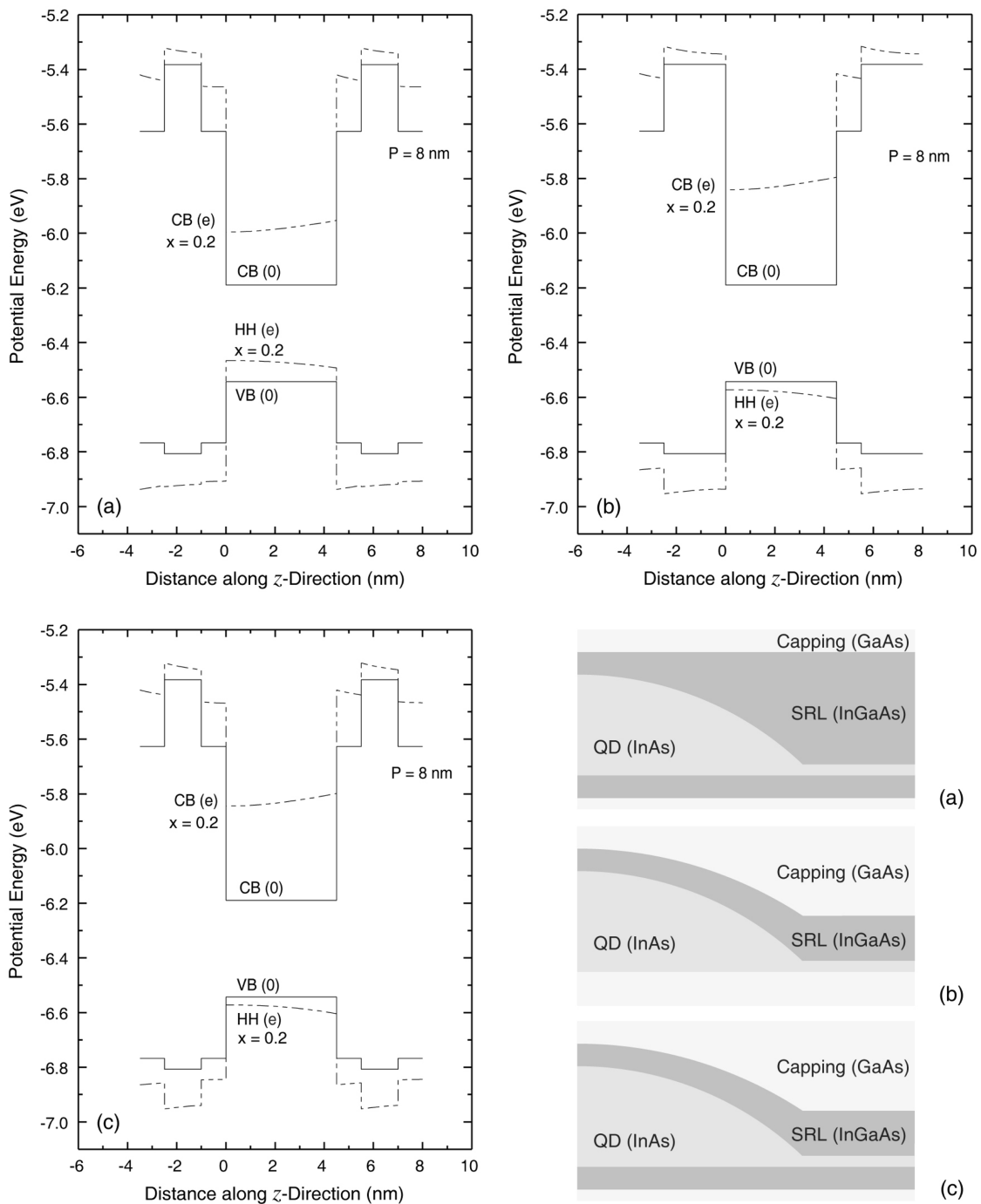


**Fig. 4.** Changes in confinement potentials with the variations in layout and SRL shape illustrated in the lower left corner with corresponding labels.

cation of the valence band by stacking period control. Although limited, additional controllability could be allowed by switching the shape of the ternary layer between a well type and a cladding type. In addition, varying the geometry (shape) of the QDs would allow some more design flexibility as inferred from previous works.<sup>[6,9]</sup> With this approach to bandgap engineering, it would be possible to vary the emis-

sion or absorption wavelengths of optoelectronic and photovoltaic devices based on InAs/GaAs QD systems for specific application purposes.

#### 4. SUMMARY AND CONCLUSIONS

Some possible routes to tailoring the optoelectronic prop-

erties of InAs/GaAs quantum dot systems were evaluated numerically. Numerical analysis predicted that when  $\text{In}_x\text{Ga}_{1-x}\text{As}$  ternary layers were introduced between the InAs QD layers, hydrostatic strains within the QD were significantly relieved with increasing In concentrations in the ternary layers, resulting mainly in the shift of the conduction band edge toward the lower energy positions yielding narrower bandgaps. Effects of the changes in the stacking period and the shape of the ternary layer were predicted to be somewhat limited. It is concluded that control of strains in QD structures *via* incorporation of InGaAs ternary layers would be an effective means of band gap engineering as it allows tailoring of the conduction band edges whereas geometry control alone may not be sufficient to achieve QD systems with a wide range of designed properties because of the limited applicability. It is therefore proposed that, if incorporation of ternary layer is combined with geometry controls such as varying stacking periods and ternary layer shapes, even greater flexibility in the tailoring of QD properties could be achieved.

#### ACKNOWLEDGMENTS

This work was supported by DAPA and ADD (W. Lee and J.-M. Myoung) and Changwon National University (W. Lee and K. Shin).

#### REFERENCES

1. P. Harrison, *Quantum Wells, Wires and Dots*, Wiley, New York (2000).
2. A. Stintz, G. T. Liu, H. Li, L. F. Lester, and K. J. A. Malloy, *IEEE Photon. Technol. Lett.* **12**, 591 (2000).
3. A. Marti, N. Lopez, E. Antolin, E. Canovas, C. Stanley, C. Farmer, L. Cuadra, and A. Luque, *Thin Solid Films* **511-512**, 638 (2006).
4. J. Phillips, K. Kamath, and P. Bhattacharya, *J. Appl. Phys.* **72**, 2020 (1998).
5. A.D. Andreev, J.R. Downes, D.A. Faux, and E.P. O'Reilly, *J. Appl. Phys.* **86**, 297 (1999).
6. M. Califano and P. Harrison, *J. Appl. Phys.* **91**, 389 (2002).
7. S.L. Chuang, *Physics of Optoelectronic Devices*, Wiley, New York, (1995).
8. E. C. Do and B.-J. Lee, *Electron. Mater. Lett.* **4**, 107 (2008).
9. H. Shin, W. Lee, and Y.-H. Yoo, *J. Phys. Condens. Matter* **15**, 3689 (2003).
10. W. Lee, J.-M. Myoung, Y.-H. Yoo, and H. Shin, *Solid State Commun.* **132**, 135 (2004).
11. S. Sauvage, P. Boucaud, J.M. Gerard, and V. Thierry-Mieg, *Phys. Rev. B* **58**, 10562 (1998).
12. J. Zou, X. Z. Liao, D. Cockayne, and R. Leon, *Phys. Rev. B* **59**, 12279 (1999).
13. J. Kim, L.W. Wang, and A. Zunger, *Phys.Rev.* **B57**, R9408 (1998).
14. J. Gere and S. Timoshenko, *Mechanics of Materials*, Chapman & Hall, London (1991).